Interacting Multiple Model Particle Filters for Side Scan Bathymetry

Augustin Alexandru Saucan, Thierry Chonavel, Christophe Sintes, Jean-Marc Le Caillec

Interacting Multiple Model Particle Filters for Side Scan Bathymetry

Augustin-Alexandru Saucan† Thierry Chonavel† Christophe Sintes† Jean-Marc Le Caillec†
{augustin.saucan, thierry.chonavel, christophe.sintes, jm.lecaillec}@telecom-bretagne.eu
† Institut Mines Telecom - Telecom Bretagne, CNRS UMR 6285 LabSTICC,
Technople Brest-Iroise - CS 83818 - 29238 Brest Cedex 3 - France

***Abstract*—In this paper we propose a multiple sea floor model based approach to improve bathymetry estimation with tracking algorithms. Traditionally interferometry is used to estimate the phase difference of signals received by two sensors, implicitly the direction of arrival *(DOA)* of the wave impinging both sensors. In our approach, we employ a state space model to describe data collected by a multi-sensor side scan sonar, and the evolution of the underlying DOA angle. The challenge with space state models is choosing the right model, and detecting the *switch* between models. We propose the use of several models that describe different sea-floor patterns and merge them within the framework of the interacting multiple model *(IMM)*. Since the sonar array processing problem is non-linear and non-Gaussian, we propose an IMM particle filter algorithm to provide robust tracking while not sacrificing performance. Also an interesting new application is the swath segmentation, which appears as a side result implied by calculating the different model probabilities.**

***Index Terms*—side scan sonar, bathymetry, DOA estimation, tracking, bootstrap filter, multiple model, IMM, Markov jump systems.**

I. Introduction

In a recent paper [1] we successfully used a DOA tracking technique for sea-floor angle of arrival estimation in the case of side scan sonars. The tracking algorithm exploits noisy array data to recover the sea-floor profile and, more importantly, to resolve multiple echoes interfering with the main sea floor echo. The multiple interfering echoes are caused by the existence of multiple paths involving sea surface reflections. Moreover, due to the non-linear and non-Gaussian state space model, the implementation of the proposed tracker was based on a particle filter, more precisely the bootstrap filter [2].

In all state space model descriptions a crucial role is played by the state equation, which represents an added prior upon the temporal evolution of the internal state. For example kynematic state models [3] such as the nearly constant velocity (*NCV*), wiener acceleration process (*WAP*) or coordinated turn (*CT*) models are employed when tracking dynamical targets. However, when dealing with maneuvering targets often one state model isn't sufficient and several multiple model (*MM*) algorithms where developed, the most popular being the *IMM*, first proposed in [4]. In our previous article, since interfering echoes were weakly structured, the internal state was chosen to be the DOA of the sea floor echo. However the problem with such an approach is that one state model cannot describe all possible terrain reliefs and corresponding angle variation. In this sense, this paper aims at presenting the adaptation and application of an IMM Bootstrap filter in the case of bathymetry tracking. The proposed algorithm is based on the IMM particle filter introduced in [5]; several batymetrical state models are employed on simulated signals and real side-scan sonar data. Also the choice of the state variable between DOA angle and bathymetric height is presented.

II. Markovian jump model for Bathymetry tracking

We consider a dynamic system with the internal state represented by the stochastic process x_t, representing either the sea floor DOA angle θ_t or the bathymetric height h_t, both being linked by a non-linear transformation. The scope is to estimate the inner state based on the system observations, represented by the stochastic process y_t, i.e. the signal received by the sensor array. let us consider equations 1 and 2, that represent the state and measurement equations of the model:

$$x_t = F_t(x_{t-1}, v_t, m_t) \tag{1}$$

$$y_t = H_t(x_t, n_t, m_t) \tag{2}$$

where t denotes the discrete time and m_t, the modal state (model) which is a time-homogeneous *(hidden)* Markov chain with M states (models). F_t and H_t represent the model conditioned transition and measurement functions and are possibly non-linear. x_t together with m_t define a *hybrid space state system* composed of euclidean and discreet valued variables. When the modal state is a Hiden Markov Chain the model is called *Markovian jump system*. The stochastic processes v and n are mutually independent white noises with known probability densities. v represents the model noise and n the measurement noise.

The Markov chain m_t dictates the model active during the time interval $]t-1, t]$, with the transition probability matrix Π defined as:

$$[\Pi]_{ij} = \pi_{ij} \triangleq P(m_t = j | m_{t-1} = i), \forall i, j \in \{1, \dots, M\} \tag{3}$$

In the context of array processing, the observation is usualy linked to the DOA angle θ_t (also indirectly to the bathymetric

height h_t) in the following way:

$$y_t = A(\theta_t)s_t + n_t \tag{4}$$

where we considered one narrow-band source located in the far-field of the uniform linear array (*ULA*) comprised of P receivers. Ideally this source signal will represent the sea floor back scattered signal. $y_t \in \mathbb{C}^{[P\times 1]}$ represents the signal received over the array. $s_t \in \mathbb{C}$ represents the source signal, $n_t \in \mathbb{C}^{[P\times 1]}$ represents the additive noise component and $A \in \mathbb{C}^{[P\times 1]}$ represents the steering vector, which is a function of the internal state. In the case of a well calibrated array, the steering vector is of the form:

$$A(\theta_t) = \begin{bmatrix} 1 \\ \exp(i2\pi\frac{d}{\lambda}\sin(\theta_t)) \\ \vdots \\ \exp(i2\pi\frac{d}{\lambda}(P-1)\sin(\theta_t)) \end{bmatrix} \tag{5}$$

where θ represents the direction of arrival of the source i.e. the back scattered sea-floor echo, d the receiver spacing and λ the wavelength. Note that θ_t is the angle between the echo DOA and the plane orthogonal to the array axis. In [1] it was shown that the observation distribution closely obeys a multivariate Laplace law [6], thus in this article we will utilize this multivariate probability distribution. Since we know the distribution of the whole observation $p(y_t)$ and not just the noise distribution $p(v_t)$ we are able to avoid the nuisance parameter s_t estimation. Furthermore the Laplace distribution proves to be robust in the sense that it yields a good overlap between the prediction pdf and the observation pdf thus making possible the application of the bootstrap filter.

The multiple model framework that we propose for bathymetry tracking is described by the jump Markov system state equation 1 and the measurement equation 4. The model state m_t is used to switch between different state prediction models either for the DOA angle or directly for the bathymetric height. The measurement equation is unaffected by m_t, however in the case of bathymetric height driven state equations an additional transformation is required.

It is well known [3], [7] that the optimal filtering algorithm in the switching multiple model framework, that is, the algorithm that recursively computes the posterior distribution $p(x_t|y_{1:t})$, requires a number of mode matched filters that *exponentially increases* with t. This branching of modes phenomenon renders impractical the optimal filter. Thus, several sub-optimal methods have been proposed. Arguably the most successful sub-optimal filter, the IMM has a distinctive similarity to the optimal filter while imposing a constant number of mode matched filters throughout the filtering process, it has M filters running in parallel [8]. If all the modes in the Markovian switching system are linear and Gaussian, each of these mode matched filters is a Kalman filter [9]. However, since the bathymetry tracking system has a non-linear and non-Gaussian measurement equation 4, we propose to use a particle implementation of the mode matched filters. The first practical particle filter, the bootstrap (*BF*) was proposed in [2] and approximates the posterior $p(x_t|y_{1:t})$ distribution with a weighted set of particles. For a thorough introduction into particle filtering methods see for instance [10].

III. IMM BF for bathymetry tracking

In this section we present the proposed IMM based particle filter aimed at estimating the internal state of the bathymetric jump Markov system. For a system comprised of M possible models, the IMM is composed of M parallel mode matched filters, each for one possible model. The probabilities of each model, $p(m_t|y_{1:t})$ are recursively computed at each time step and used to merge the individual filter estimates. The mode matched filters are implemented using a bootstrap filter, with each filter having its own set of particles, as opposed to the single shared set implementation proposed in [11], also presented into more details in [12]. The IMM algorithm is generically decomposed into 4 stages: mixing, model conditional filtering, model probability update and merging of individual filter estimates. The proposed IMMBF algorithm is illustrated in Algorithm 1.

The key step of the IMM algorithm is the mixing stage, where the input of each mode matched filter j at time instant t is obtained from the *mixing* of the mode matched filter estimates from time instant $t-1$, effectively achieving an *interaction* of the M models. The weightings used to perform the mixing are called mixing probabilities, $\mu^{i|j}$ and are defined as the probability that mode i was in effect at time $t-1$ given that model j is in effect at time t. In the case of linear-Gaussian systems the mixing distribution $p(x_t|m_t = j, y_{1:t})$ is a weighted sum of Gaussian distributions with the weights $\mu^{i|j}$ [3]. Note that the original IMM approximates the mixing distribution by a single Gaussian with the same mean and covariance as the Gaussian mixture. When dealing with non-linear and non-Gaussian systems, Monte Carlo approximations of distributions as weighted particles are employed [13]. In such conditions, the mixing distribution for $m_t = j$ is obtained by sampling from the $\mu^{i|j}$ weighted sum of model matched posterior densities obtained at $t-1$, $\sum_i \mu^{i|j} p(x_{t-1}|m_{t-1} = i, y_{1:t})$.

The mixing distribution computed for each model j is utilized to reinitialize the mode matched particle filters in the model conditioned filtering step. Furthermore filtering is carried out in the usual two step procedure: prediction of the reinitialized particles through the state transition equation 1 and weights updating of the reinitialized particles taking into account the new observation. We only perform resampling when *effective number of particles* drops below a threshold value [14]. At the end of this step the mode conditioned posterior distribution $p(x_t|m_t = j, y_{1:t})$ is obtained for each mode j as a weighted particle approximation.

The model conditioned likelihoods $p(y_t|x_t^{(n)j})$ computed for each particle (n) and model j are utilized to update the model probabilities. As suggested in [15] we consider an average model likelihood L_t^j as the mean of the individual particles likelihoods in each of the models. Based on the newly computed model probabilities the overall posterior density $p(x_t|y_{1:t})$ is estimated as the weighted sum of the model conditioned posterior distributions $p(x_t|m_t = j, y_{1:t})$. This operation is again achieved by sampling.

Algorithm 1: IMM Bootstrap Filter (IMMBF).

for $j = 1$ **to** M **do**

1. Mixing or model conditional reinitialization

Predicted mode probability: $\mu^j_{t|t-1} \triangleq P(m_t = j|y_{1:t-1}) = \sum_i \pi_{ij}\mu^i_{t-1}$

Mixing weight: $\mu^{i|j} \triangleq P(m_{t-1} = i|m_t = j, y_{1:t-1}) = \pi_{ij}\mu^i_{t-1}/\mu^j_{t|t-1}$

Mixing density: $p(x_{t-1}|m_t = j, y_{1:t-1}) = \sum_i \mu^{i|j} p(x_{t-1}|m_{t-1} = i, y_{1:t-1})$

Sample $\{(x^{(n)}_{t-1|m_t=j}, w(x^{(n)}_{t-1|m_t=j}))_{n=1,\dots,N}\} \sim p(x_{t-1}|m_t = j, y_{1:t-1})$

2. Model conditional filtering

for $n = 1$ **to** N **do**

Particle propagation: $\tilde{x}^{(n)j}_t \sim p(x_t|x^{(n)}_{t-1|m_t=j}, m_t = j)$

Particle likelihood: $q^{(n)j}_t = p(y_t|\tilde{x}^{(n)j}_t)$

Particle weight update: $w(\tilde{x}^{(n)j}_t) = q^{(n)j}_t w(x^{(n)}_{t-1|m_t=j})$

end

Compute mode likelihood: $L^j_t = \frac{1}{N}\sum_n q^{(n)j}_t$

Normalize particle weights: $\tilde{w}^{(n)j} = \frac{w(\tilde{x}^{(n)j}_t)}{\sum_n w(\tilde{x}^{(n)j}_t)}$

Compute effective number of samples: $N^j_{eff} = \frac{1}{\sum_n \tilde{w}^{(n)j}}$

if $N^j_{eff} < N_{thresh}$ **then**

Resample $\{(\tilde{x}^{(n)j}_t, \tilde{w}^{(n)j})_{n=1,\dots,N}\}$ *to obtain* $\{(x^{(n)j}_t, w^{(n)j} = \frac{1}{N})_{n=1,\dots,N}\}$

else

$\{(x^{(n)j}_t, w^{(n)j})_{n=1,\dots,N}\} = \{(\tilde{x}^{(n)j}_t, \tilde{w}^{(n)j})_{n=1,\dots,N}\}$

end

end

3. Model Probability update

for $j = 1$ **to** M **do**

Mode probability: $\mu^j_{t|t} \triangleq P(m_t = j|Y_{1:t}) = \frac{\mu^j_{t|t-1}L^j_t}{\sum_{i=1}^M \mu^i_{t|t-1}L^i_t}$

end

4. Model merging

Overall MMSE estimate: $\hat{x}_{t|t} \triangleq \mathbb{E}\{x_t|y_{1:t}\} \approx \sum_{j=1}^{M} \mu^j_t \sum_{n=1}^{N} x^{(n)j}_t w^{(n)j}$

IV. RESULTS: SIMULATION AND REAL SONAR DATA

A. Simulated underwater scene

The simulated underwater scenario is used to assess the ability of the IMMBF algorithm to detect *jumps*, i.e. model changes in the DOA angle evolution and to track the bathymetry. Thus two models for the bathymetric height were envisaged: a random walk model, *RW* and a nearly constant slope *NCS*, defined in a similar fashion as the nearly constant velocity model for dynamical targets. The idea behind the two is that the NCS model is intended to describe flat smooth regions with unknown inclination angles and the RW model is intended for rough, i.e. non-smooth areas. The IMMBF consisted of $N = 100$ particles in each model. The initial model probabilities and the transition matrix are given by:

$$\mu_0 = \begin{bmatrix} 0.5 \\ 0.5 \end{bmatrix} \qquad \Pi = \begin{bmatrix} 0.98 & 0.02 \\ 0.02 & 0.98 \end{bmatrix}. \tag{6}$$

The state variable x_t is composed of the bathymetric height and it's derivative with respect to the slant range r_S. $\Delta_S = cT_s/2$ represents the range bin width, T_s the sampling period and c the celerity.

$$x_t = \begin{bmatrix} h_t & \frac{\partial h_t}{\partial r_S} \end{bmatrix}^T \tag{7}$$

The model transition functions are given by:

$$F(x_{t-1}, v_t, 1) = F_{RW}x_{t-1} + v^{RW}_t \tag{8}$$

$$F(x_{t-1}, v_t, 2) = F_{NCS}x_{t-1} + \Gamma v^{NCS}_t \tag{9}$$

$$F_{NCS} = \begin{bmatrix} 1 & \Delta_S \\ 0 & \frac{\Delta_S^2}{2} \end{bmatrix}, \quad \Gamma = \begin{bmatrix} \frac{\Delta_S^2}{2} \\ \Delta_S \end{bmatrix}, \quad F_{RW} = \begin{bmatrix} 1 & 0 \\ 0 & 0 \end{bmatrix} \tag{10}$$

v_t^{RW} and v_t^{NCS} are white zero mean Gaussian sequences with standard deviations σ_{RW} and σ_{NCS} and represent a bathymetric height noise and a height "acceleration" noise sequence. The simulated underwater scene is presented in Fig. 1 and represents the swath bathymetric profile of one ping line. The tilted sonar array is located $15m$ above the sea-floor, which exhibits a flat and smooth surface except for a *rough* patch, a fluctuation of the sea-floor height. Since the scenario is intended only for the *switching* of models, there is no shadow effects simulated on the backscattered signal. However noise is added to the backscattered signal and the SNR, signal to noise power ratio is considered to drop from $30dB$ to $10dB$ along the swath width accounting for the wave spherical spreading effect. Also in Fig. 1 we present in detail the *rough* patch and also the estimates obtained with the IMMBF algorithm.

In Fig. 2 we compare the angular pseudo-spectrum obtained with MUSIC [16], the sea-floor profile and the estimated probabilities of both models, RW and NCS, obtained with the IMMBF algorithm. The effect of the rough patch on the DOA of the backscattered wave can be seen in a detail of the pseudo-spectrum, however, affected by the averaging of the MUSIC algorithm. As expected, we observe that the model active in the flat regions of the sea-floor is the NCS model, while the RW is active in the rough patch area. The IMMBF algorithm successfully detects the switch (jump) of the model best suited to describe the sea-floor height evolution. The variances were set to $\sigma_{RW} = 1m$ and $\sigma_{NCS} = 1m^{-2}$. Although some design considerations should be taken into account when choosing the value of these variances, the detection of the model jumps was found to be robust for values within the chosen order. The ability of the IMMBF algorithm to detect model jumps is not only important for improving the estimates by using the locally best adapted model but considering the model probability vector also provides an information about the sea-floor's nature: segmenting the swat into the classes determined by the models.

Similar results were obtained, in terms of *model jump* detection, with two random walk sea-floor models with standard deviations: $\sigma_{RW1} = 0.01m$ and $\sigma_{RW1} = 1m$. The first model describes a smoother surface while the second one describes a rougher surface; coupled with the IMMBF they achieve basically the same segmentation, as shown in Fig. 2.

B. Real side-scan sonar data

The IMMBF algorithm was also tested on data issued from a bathymetric side-scan sonar. The sonar receiving arrays are composed of 8 staves allowing for bathymetry reconstruction as well as classical imagery. The data was collected in a survey of a shallow water harbor, with a relatively flat floor at depth varying around $15m$. This particular combination of shallow water, calm sea and pole mounted sonar causes the apparition of multi-path echoes in the angular spectrogram, as shown in Fig. 3 and reference [1]. The spectrogram in Fig. 3 was obtained with the MVDR or Capon beamformer [17], and superimposed on this image are the IMMBF estimates. Let us notice the similarity of the DOA arch-like curve similar with the one in Fig. 2 that is typical of a relatively flat sea-bottom.

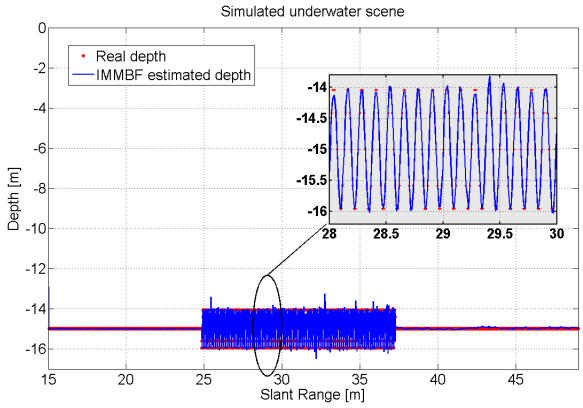

Fig. 1. Simulated underwater scene and detail of rough patch.

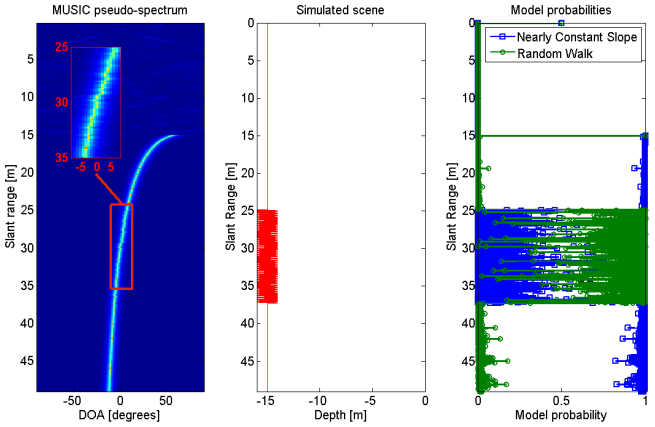

Fig. 2. Comparison of angular spectrum, sea-floor profile and IMMBF model probabilities.

We used a two model Markovian switching system with model transition matrix and initial probabilities given by 6. For the implementation, we used again $N = 100$ particles in each model. However both models are angular random walk models with different model noises.

$$x_t = \theta_t \tag{11}$$

$$F(x_{t-1}, v_t, m_t \in \{1, 2\}) = x_{t-1} + v_t^{m_t} \tag{12}$$

where θ_t represents the DOA angle, $v_t^{m_t}$ is white zero mean Gaussian noise sequences with variance σ_{m_t}. The first model has a constant standard deviation $\sigma_1 = 0.1^\circ$ and the second one has a time varying standard deviation $\sigma_2 = f(t)$, starting with 0.1° at the beginning of the swath and increasing linearly to 2° at the end of the swath width.

In Fig. 4 we present the IMMBF estimated probabilities for both models. At the beginning of the swath width the second model is better adapted to describe the evolution of the bathymetry. Indeed the DOA angle has a faster changing rate at the beginning of the swath than at the end of the swath and the first model with its small variability does not cope well at small range values. However, it offers better estimates at bigger ranges. To better illustrate the model choice, in Fig. 5 we present the particle clouds of both models. In each mode

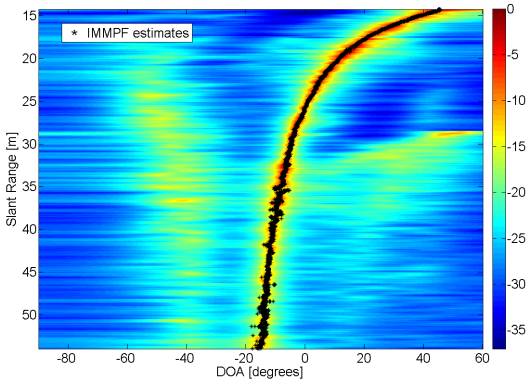

Fig. 3. Capon angular spectrum and IMMBF DOA estimates.

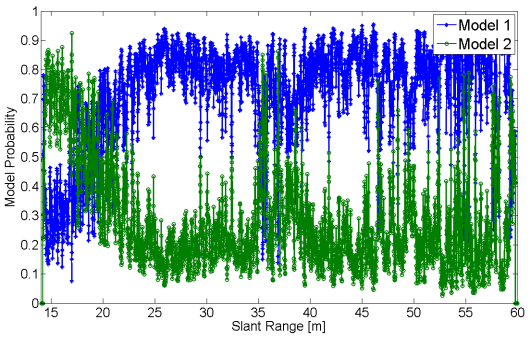

Fig. 4. IMMBF model probabilities.

and at each range bin, there are 100 particles, i.e. angular positions, which together with their associated weights form the empirical posterior density. Although the particle positions are not enough to characterize the variance of particles inside each mode, they offer a visual interpretation of the *fluctuation* in each mode. Also in Fig. 5 around the $35m$ range mark we can observe a sudden increase in particle fluctuation in both of the models. This is caused by a discontinuity of the DOA curve and its effect is also visible in Fig. 4 with a short-transient jump in the model probabilities. Such discontinuities, generally caused by shadows, correspond to an absence of signal and need to be detected beforehand since tracking should not be conducted over shadows.

V. Conclusion and perspectives

This paper presents the application of the IMMBF algorithm to simulated and real side-scan sonar data. At the price of increased complexity, multiple model algorithms offer the possibility of robust tracking when the models used to track the dynamics of the target are relevant. The simulated and real data experiments show the potential interest of multiple model algorithms for bathymetry enhancement. Also a new and interesting application, which will be further investigated is the swath segmentation.

VI. Acknowledgment

This work was funded by a grant of *Direction Générale d'Armement* (French MoD) and the Carnot Institute.

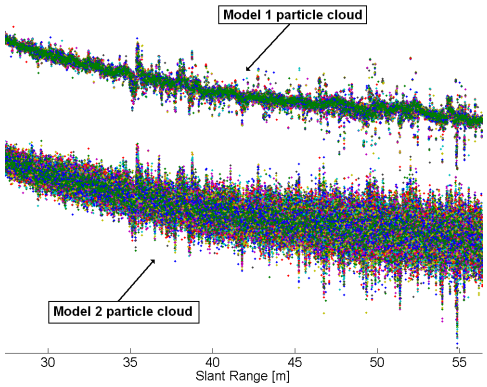

Fig. 5. Particle clouds for both models.

References

[1] A. A. Saucan, C. Sintes, T. Chonavel, and J. M. Le Caillec, "Enhanced sonar bathymetry tracking in multi-path environment," *IEEE Oceans Conference Hampton Roads*, 2012.

[2] N. Gordon, D. Salmond, and A. Smith, "Novel approach to nonlinear/non-gaussian bayesian state estimation," *IEEE Proceedings F, Radar and Signal Processing*, vol. 140, pp. 107–113, 1993.

[3] Y. Bar-Shalom, X. Rong Li, and T. Kirubarajan, *Estimation with Applications to Tracking and Navigation: Algorithms and Software for Information Extraction.* Jhon Wiley and Sons, 2001.

[4] H. A. P. Blom and Y. Bar-Shalom, "The interacting multiple model algorithm for systems with markovian switching coefficients." *IEEE Transactions on Automatical Control*, vol. 33, no. 8, pp. 780–783, August 1988.

[5] Y. Boers and J. Driessen, "Interacting multiple model particle filter," *IEE Proceedings - Radar, SOnar and Navigation*, vol. 150, no. 5, pp. 344–349, October 2003.

[6] T. Eltoft, T. Kim, and T. Lee, "On the multivariate laplace distribution," *IEEE Signal Processing Letters*, vol. 13, no. 5, pp. 300–303, May 2006.

[7] B. Ristic, S. Arulampalam, and N. Gordon, *Beyond the Kalman Filter: Particle filters for Tracking Applications*. Artech House, 2004.

[8] Y. Bar-Shalom, S. Challa, and H. A. P. Blom, "IMM estimator versus optimal estimator for hybrid systems," *IEEE Transactions on Aerospace and Electronic Systems*, vol. 41, no. 3, pp. 986–991, July 2005.

[9] R. Kalman, "A new approach to linear filtering and prediction problems," *Transactions of the ASME - Journal of Basic Engineering*, vol. 82, pp. 35–45, 1960.

[10] J. Candy, *Bayesian Signal Processing: Classical, Modern and Particle Filtering Methods.* Hoboken, N.J.: Wiley/IEEE Press, 2009.

[11] S. McGinnity and G. W. Irwin, "Multiple model bootstrap filter for maneuvering target tracking," *IEEE Transactions on Aerospace and Electronic Systems*, vol. 36, no. 3, pp. 1006–1012, July 2000.

[12] A. Doucet, N. de Freitas, and N. Gordon, *Sequantial Monte Carlo Methods in Practice*. New York: Springer-Verlag, 2001.

[13] A. Doucet and X. Wang, "Monte carlo methods for signal processing: A review in the statistical signal processing context," *IEEE Signal Processing Magazine*, vol. 22, pp. 152–170, November 2005.

[14] J. Liu and R. Chen, "Sequential monte carlo methods for dynamical systems," *Jurnal of American Statistical Association*, vol. 93, pp. 1032–1044, 1998.

[15] H. Driessen and Y. Boers, "Efficient particle filter for jump markov nonlinear systems," *IEE Proceedings - Radar, Sonar and Navigation*, vol. 152, no. 5, pp. 323–326, October 2005.

[16] R. O. Schmidt, "Multiple emitter location and signal parameter estimation," *IEEE Transactions on Antennas and Propagation*, vol. 34, no. 3, pp. 276–280, March 1986.

[17] J. Capon, "High-resolution frequency-wavenumber spectrum analysis," *Proceedings of the IEEE*, vol. 57, no. 8, pp. 1408 – 1418, August 1969.